Available online at www.sciencedirect.com
ScienceDirect
Remote Sensing of Environment 107 (2007) 45–53
Remote Sensing of Environment
www.elsevier.com/locate/rse

Comparison of MISR aerosol optical thickness with AERONET measurements in Beijing metropolitan area

Xin Jiang [a,*], Yang Liu [b], Bin Yu [c], Ming Jiang [a]

[a] *LMAM, School of Mathematical Sciences, Peking University, Beijing 100871, China*
[b] *Harvard School of Public Health, Boston, MA 02215, U.S.*
[c] *Department of Statistics, University of California, Berkeley, CA 94720–3860, U.S.*

Received 28 February 2006; received in revised form 7 June 2006; accepted 10 June 2006

Abstract

Aerosol optical thickness (AOT) data retrieved by the Multi-angle Imaging SpectroRadiometer (MISR) from 2002 to 2004 were compared with AOT measurements from an Aerosol Robotic Network (AERONET) site located in Beijing urban area. AERONET AOT data were first averaged within a two-hour time window and MISR data were collected using AOTs of the central regions covering the AERONET site and the average AOTs of the surrounding 3×3 regions. MISR and AERONET AOTs are highly correlated, with an overall linear correlation coefficient of 0.93 at 558 nm wavelength. On average, MISR AOT at 558 nm is 29% lower than the AERONET AOT at 558 nm interpolated from 440 nm and 675 nm. A linear regression analysis using MISR AOT as the response yields a slope of 0.58 ± 0.03 and an intercept of 0.07 ± 0.02 in the green band with similar results in the other three bands, indicating that MISR may underestimate AERONET AOT. After applying a narrower averaging time window to AERONET data and controlling their temporal variabilities, the agreement between MISR and AERONET AOTs is significantly improved with the correlation coefficient of 0.97 and a slope of 0.71 ± 0.03 in an ordinary linear least squares fit. A weighted linear least squares, which reduces the impact of spatial averaging, yields a better result with the slope going up to 0.73 ± 0.03. When only the central region MISR AOTs are included in the regression analysis, the best agreement is achieved with a slope of 0.91 ± 0.03 and an intercept of 0.00 ± 0.01, and MISR AOT is only 9% lower than AERONET AOT on average. By investigating PM_{10} spatial distribution of Beijing, we found substantial spatial variations of aerosol loading with higher PM_{10} concentrations in the MISR central region, which introduced low bias in validating spatial average MISR AOT. When MISR and AERONET AOT are better spatiotemporally matched, their agreement can be much better than the previously reported results. Our findings also suggest that MISR aerosol retrieval algorithm might need to be adjusted for the extremely high aerosol loadings and substantial spatial variations that it will probably encounter in heavily polluted metropolitan areas.

Keywords: MISR; Aerosol optical thickness; AOT; AERONET; PM_{10}; Correlation; Ordinary least squares; Weighted least squares

1. Introduction

Atmospheric aerosols affect our environment from global to regional to local scale. On global and regional scales, their impacts on Earth radiation budget and cloud microphysics are considered a major uncertainty in climate change. Ground level aerosols, also known as particulate matter (PM), have been associated with multiple adverse health effects (Pope et al., 1995). Many countries in the world have designated PM as a criteria air pollutant. Therefore, long term PM monitoring has been of importance, especially for those heavily polluted locations.

The Multi-angle Imaging SpectroRadiometer (MISR), aboard the NASA's Earth Observing System (EOS) Terra satellite, provides global information on tropospheric aerosol properties. Viewing the sunlit Earth almost simultaneously at nine angles along its track, MISR obtains 4-spectral (446, 558, 672 and 866 nm) imagery at 1.1 km spatial resolution in the non-red bands and 275 m resolution in the red band. It has a periodic coverage between two and nine days depending on the latitude (Diner et al., 1998; Martonchik et al., 2002). MISR's unique combination of multiple bands and angles enables it to retrieve aerosol optical thickness (AOT) and additional particle

* Corresponding author. Tel.: +86 10 58876470.
E-mail address: jiangxin@pku.edu.cn (X. Jiang).

0034-4257/$ - see front matter © 2006 Elsevier Inc. All rights reserved.
doi:10.1016/j.rse.2006.06.022

properties at a resolution of 17.6 km over both land and ocean, with no assumption about the absolute land surface reflectance or its spectral characteristics in the aerosol retrieval algorithm (Martonchik et al., 2002, 1998).

Generally, MISR AOT retrieval is validated by comparing with ground-based sun photometer measurements. The Aerosol Robotic Network (AERONET) is a worldwide network of automatic sun photometers and data archive, providing spectral aerosol optical thickness as well as aerosol microphysical properties (Holben et al., 1998). Due to their relatively high accuracy (AOT uncertainty < ±0.01 at wavelengths > 440 nm), AERONET data have been widely used as a standard for validating satellite aerosol retrievals (Dubovik et al., 2000; Holben et al., 1998).

Early MISR AOT data (prior to version 15) have been validated under various scenarios. Diner et al. (2001) for the first time compared the MISR AOT with AERONET over southern Africa from the August to September 2000, showing that MISR AOT compare favorably with AERONET with a positive bias of 0.02 and an overestimation of 10%. Liu et al. (2004b) conducted a validation based on 16 AERONET sites over the United States, and found a good agreement between the MISR and AERONET AOTs after two outliers were excluded (linear regression analysis using MISR AOT as the response variable yielded an R^2 of 0.80, a slope of 0.88 and an intercept of 0.04). Good agreement was also obtained in the desert regions, where the surface reflectance is high (Christopher and Wang, 2004; Martonchik et al., 2004). In Abdou et al. (2005), AOT retrieved by both the Moderate Resolution Imaging SpectroRadiometer (MODIS) and MISR were both compared with AERONET to explore the similarities and differences between them, and result showed MISR has a lower bias than MODIS over land (regression result: MISR = 0.83 × AERONET + 0.03, r = 0.86). Kahn et al. (2005) conducted a comprehensive global validation of MISR AOT using two years of MISR and AERONET AOT data, stratified by season and expected aerosol type. Detailed analyses were made on the likely causes for the trends and outliers to improve the MISR aerosol retrieval algorithm. It should be noted that validation of the MISR aerosol product is still underway, and the retrieval algorithm is still being refined.

Although Kahn et al. (2005) covered three polluted urban sites, i.e., Mexico City, Kanpur in northern India, and Shirahama in southern Japan, the AOT values at these sites are substantially lower than those found in Beijing as shown in the current analysis. Beijing is one of the largest metropolitan areas in the world. Studies have demonstrated that the aerosol loading is extremely high in the urban areas of Beijing (Eck et al., 2005). Traditionally, the major particle emission sources consist of industrial emissions, coal burning for winter heating and power supply, and long-range transported dust. In recent years, traffic emission has become a major contributor to the severe air pollution in Beijing, making the particle composition more complex and variable (He et al., 2001; Sun et al., 2004). This study is to assess MISR AOT quality in Beijing using information from AERONET, and analyze the likely causes of the MISR–AERONET discrepancies. In addition, because of the rapid economic growth and urbanization, air pollution has become a serious problem for Beijing. Several pollution-control measures have been deployed since 1990 s, such as natural gas substitution to coal and use of low-sulfur coal. However, inhalable particles (PM_{10}, particles smaller than 10 μm in aerodynamic diameter) pollution is still at a level higher than the Chinese national ambient air quality standard. It has been demonstrated that satellite remote sensing aerosol products, such as MISR AOT, combined with the surface monitoring networks, can provide a cost-effective way to monitor and forecast air quality (Chu et al., 2003; Liu et al., 2004a, 2005). Therefore, it is also a motivation of this study to explore the application of satellite remote sensing in monitoring pollution in China.

The rest of the paper is organized as follows. In Section 2, we describe the data used in the current study. In Section 3, we first summarize the matched MISR and AERONET AOT data, and then we use various statistical tools to study the impacts of the averaging time window of AERONET AOT and the spatial averaging of MISR AOT on the agreement between AERONET and MISR AOT values. In addition to the analysis of MISR and AERONET AOT data, we also examine the spatial variability of ground-level PM mass concentrations as an indicator of the particle loading in the air column. The final section summarizes the results and draws the conclusions.

2. Data

We downloaded the AERONET level 2 (quality assured) data of the AERONET Beijing site from April 2002 to October 2004 from the AERONET data archive (http://aeronet.gsfc.nasa.gov). This site is at the Institute of Atmospheric Physics (IAP), Chinese Academy of Sciences, which is located in densely populated urban area of Beijing. A sun photometer (Cimel Electronique, France) at this site was installed on the roof of the IAP building (39.98°N, 116.38°E, and 30 m above the ground, shown in Fig. 1). Data provided by AERONET include AOT values recorded every 15 min in seven spectral bands (340, 380, 440, 500, 670, 870 and 1020 nm), Angstrom exponents, single scattering albedos and sampling dates and times. AERONET AOT at 440 nm and 670 nm were interpolated to 558 nm using Angstrom exponent ($\alpha_{440-670\ nm}$) provided by AERONET in order to compare with MISR AOT value at green band.

The MISR level 2 aerosol data (version 15) were downloaded from the NASA Langley Research Center Atmospheric Sciences Data Center (http://eosweb.larc.nasa.gov/PRODOCS/misr/table_misr.html). In this analysis, we used data covering the same period and geographic location as the AERONET Beijing site. The MISR AOT parameter used in this study is the regional mean AOT (MISR parameter name: RegMeanSpectralOptDepth), which is computed as the unweighted mean of optical thicknesses of all successful aerosol models in the retrieval algorithm (Jet Propulsion Laboratory (JPL), 2004). This is the recommended parameter by the MISR team among the AOT parameters (best fit AOT, regional mean AOT and weighted regional mean AOT) (Abdou et al., 2005). It was shown that the three MISR AOT parameters in early versions of MISR data were highly comparable (Liu et al., 2004b). Regional mean single scattering albedo (MISR parameter name: RegMeanSpectralSSA) were also extracted.

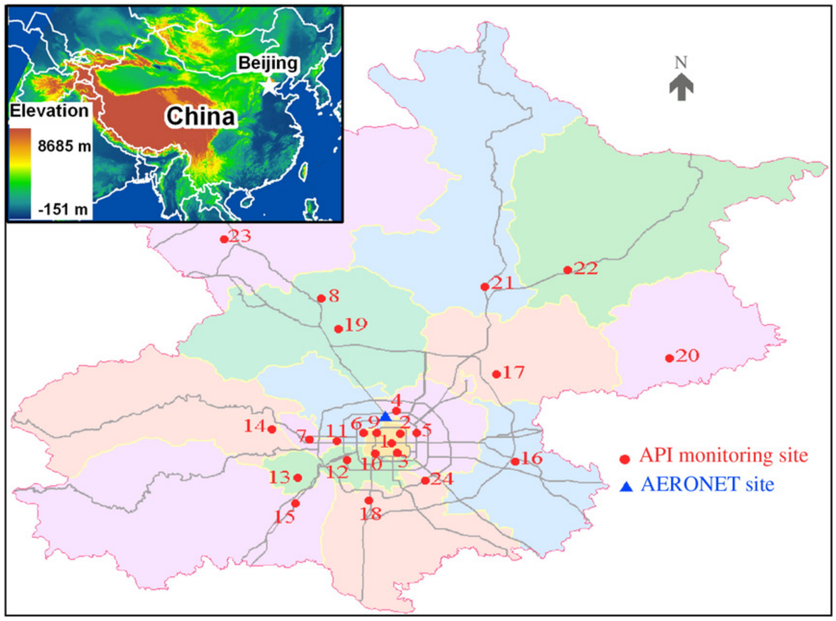

Fig. 1. The map of Beijing and locations of AERONET site (blue triangle) and API/PM_{10} monitoring sites (red dots). The API sites are numbered as follow: (1) Qianmen, (2) Dongsi, (3) Tiantan, (4) Olympic Center, (5) Nongzhanguan, (6) Chegongzhuang, (7) Gucheng, (8) Dingling, (9) Guanyuan, (10) Wanshougong, (11) Yuquanlu, (12) Fengtaizhen, (13) Yungang, (14) Longquanzhen, (15) Liangxiangzhen, (16) Tongzhouzhen, (17) Renhezhen, (18) Huangcunzhen, (19) Changpingzhen, (20) Pingguzhen, (21) Huairouzhen, (22) Miyunzhen, (23) Yanqingzhen and (24) Yizhuang. The solid gray lines represent the major roads of Beijing.

In this paper, spatially and temporally matched MISR–AERONET AOT measurement points, i.e., pairs of MISR–AERONET AOT values, were acquired by following the method described in Kahn et al. (2005). For those 17.6×17.6 km regions containing the AERONET site, successfully retrieved AOTs were directly taken and denoted as "central" points; otherwise the averages of all successful retrievals of eight surrounding regions were used instead and denoted as "surrounding" points. Fig. 2 indicates the central and surrounding regions by the white square in a 2-D MISR AOT image. Beijing as well as the densely populated industrial areas to its south and east is bordered by the low mountains (500–1500 m above sea level) to the north and west. These mountains together with the relatively low and persistent inversion layer over Beijing area effectively trap local emissions and cause the distinctive regional pattern of AOT and severe air pollution as shown in Fig. 2. AERONET data were also averaged within a fixed two-hour window between 2:00 and 4:00 UTC time, which covers the MISR overpass time. However, MISR measures instantaneous AOT over the area of a region, while the matched AERONET data actually give temporally averaged AOT at a surface point. Therefore, this inherent difference may introduce discrepancy between the two sets of data, especially in the situation of large spatial or temporal variations.

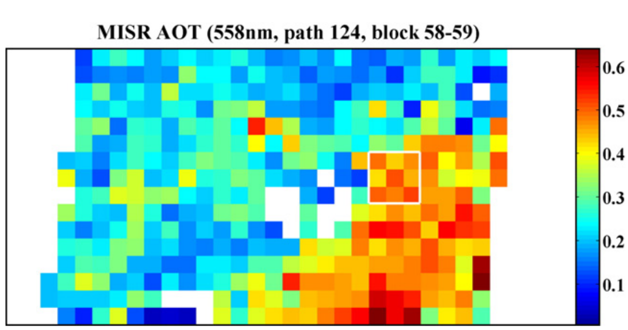

Fig. 2. 2-D map of the three-year average (Apr. 2002 to Oct. 2004) MISR AOT (path 124 and block 58–59). Path 124 is one of the six MISR paths (120–125) traversing Beijing. The 3×3 MISR region that covers the AERONET site in Beijing are marked by the white square.

It has been shown that MISR AOT is mostly sensitive to particles between 0.1 and 2 μm (Kahn et al., 1998), which roughly corresponds to the size range of fine particulate matters ($PM_{2.5}$). However, long-term $PM_{2.5}$ monitoring data is not available in Beijing. In order to investigate the aerosol spatial distribution in Beijing and its impact on MISR–AERONET agreement, two years of Air Pollution Indices (API) from 24 monitoring sites spreading over Beijing (Fig. 1) were obtained from Beijing Environmental Protection Bureau website (http://www.bjepb.gov.cn). Then the APIs were converted to daily mean PM_{10} concentrations by a piecewise linear transformation (http://www.sepa.gov.cn/quality/background.php).

3. Results and discussion

This section contains our analysis of the data described in Section 2. We start with exploratory data analysis through summary statistics, data stratification into years and seasons, and data visualization of time series plots. We then study the impact of aerosol temporal and spatial variability on the agreement between MISR and AERONET AOT values using scatterplots, simple linear regression, weighted linear regression, and difference analysis. Finally, we analyze the heterogeneity of aerosol loading as shown by the ground-level PM_{10} concentrations measured in Beijing.

3.1. Summary statistics

A total of 80 matched MISR–AERONET AOT measurement points were obtained, including 48 central points and 32 surrounding points. One potential outlier, where the AERONET AOT value at 558 nm equaled 3.83, was eliminated from the following analysis, because the current MISR aerosol retrieval algorithm discards all AOT values greater than 3.0. Summary statistics for overall and stratified matched MISR and AERONET green band AOT values are presented in Table 1. On average, both AERONET and MISR AOT are at least twice as large as those found in previous MISR validation analyses (Diner et al., 2001; Kahn et al., 2005; Liu et al., 2004b). Over all, the correlation between MISR and AERONET AOT is very strong (Pearson's linear correlation coefficient $r=0.93$), but on average MISR is approximately 29% lower (This relative difference is computed as (mean(AERONET) − mean(MISR))/mean(AERONET)). Approximately 56% of the MISR AOT values fall within the expected uncertainty envelope: 0.05 or 20%×AERONET AOT, whichever is larger (theoretically derived AOT uncertainties over calm ocean) (Kahn et al., 2001).

The percentage of MISR AOT falling in the expected uncertainty range increases over the years probably due to the overall decreasing trend in matched AOT values. It should be noted that Fig. 3a indicates that AERONET AOT level is about the same as in the calendar years 2002 and 2003 (annul average AOT=0.66), while slightly lower in 2004 (annul average AOT=0.55). Thus, the decreasing trend observed in the matched AOT values is probably because some episodes of high aerosol loadings observed by AERONET were not captured by the matched measurements.

Table 1
Summary statistics of MISR and AERONET AOT at 558 nm

Year/season (sample size)[a]	AERONET mean±std[b]	MISR mean±std	Regression slope; intercept[c]	Correlation coefficient	MISR AOT within expected uncertainty[d], %
Total (79)[e]	0.55±0.58	0.39±0.36	0.58; 0.07	0.93*	56
2002 (15)	0.74±0.64	0.56±0.37	0.53; 0.17	0.92*	40
2003 (35)	0.61±0.57	0.40±0.36	0.59; 0.04	0.92*	57
2004 (29)	0.39±0.50	0.30±0.31	0.60; 0.07	0.95*	62
Winter (18)	0.23±0.18	0.18±0.12	0.44; 0.07	0.70**	61
Spring (21)	0.54±0.48	0.44±0.29	0.55; 0.14	0.91*	57
Summer (26)	0.84±0.74	0.58±0.47	0.59; 0.08	0.95*	50
Autumn (14)	0.44±0.39	0.27±0.19	0.42; 0.08	0.87*	57

[a] Winter is December through February, spring is March through May, summer is June through August, and fall is September through November.
[b] Std refers to arithmetic standard deviation.
[c] Linear regression analysis: MISR AOT is the response variable, and AERONET AOT is the explanatory variable.
[d] MISR uncertainty envelope: the maximum of ±0.05 or 20%×AOT of AERONET.
[e] One potential outlier is excluded.
* Significant at the $\alpha=0.01$ level.
** p-value=0.013.

A strong seasonal pattern is clearly shown in the matched AOT data with higher AOT values in the spring and summer and lower AOT values in the autumn and winter (Fig. 3b). There are frequent occasions in the spring and summer when AOT values are greater than 1.5. The MISR AOT closely follows the temporal variation of AERONET AOT although it is often lower than AERONET measurements at very high AOT values. Summer has the highest AOT level among four seasons, primarily because of the increased secondary particle generation due to strong solar radiation, low wind speed and high relative humidity (Li, 2002). Sand storms are an important contributor to the high AOT levels in springtime. Correlation between AERONET and MISR AOT is very strong in the summer ($r=0.95$), spring ($r=0.91$) and autumn ($r=0.87$). Regression results show MISR AOT compares worse with AERONET AOT in the winter ($r=0.70$, regression slope=0.44), it is possibly because winter heating substantially increase coal-burning emissions in entire northern China including Beijing, resulting in more light-absorbing particles (black carbon) in the air. An investigation of the single scattering albedo (SSA) from AERONET data shows that particles commonly have SSA values around 0.88 at 672 nm in the winter, whereas the averaged MISR SSA during the same period is 0.97. A statistical hypothesis testing confirms that the mean of AERONET is significantly lower than that of MISR. This indicates that the current MISR retrieval algorithm might lack appropriate aerosol models with sufficiently low single scattering albedos to characterize this type of polluted air observed in Beijing.

3.2. Linear regression and differences analysis

The summary statistics and time series plots show a consistent underestimation of AOT by MISR when compared with AERONET, especially at high AOT values. It might be caused by the lack of appropriate aerosol models in the MISR aerosol retrieval algorithm, or by other factors such as the temporal and spatial variabilities of aerosols. Next we use various statistical tools to study these possible causes of this underestimation.

The scatterplots of MISR versus AERONET AOTs in all four MISR bands are shown in Fig. 4. The dashed lines represent the 1:1 line and the MISR expected uncertainty envelope, while the vertical and horizontal error bars on each point represent the spatial and temporal standard deviations due to spatial and temporal averaging. Regressing MISR AOT against AERONET AOT yields an R^2 of 0.87 and an RMSE of 0.13 in MISR green band. The regression slope of 0.58 ± 0.03 as well as the intercept of 0.07 ± 0.02 indicates that MISR substantially underestimates the AERONET AOT. Overall, the four bands show similar trends, with R^2 ranging from 0.84 to 0.87. Regression slopes increase slightly with wavelengths (slope=0.51, 0.58, 0.60, 0.64 in four MISR bands), but they are still significantly lower than those reported in previous MISR–AERONET comparisons. It is unlikely that interpolation of AERONET AOT values at 440 and 670 nm introduced substantial errors into the AERONET 558 nm AOT values. From now on, our analysis focuses on

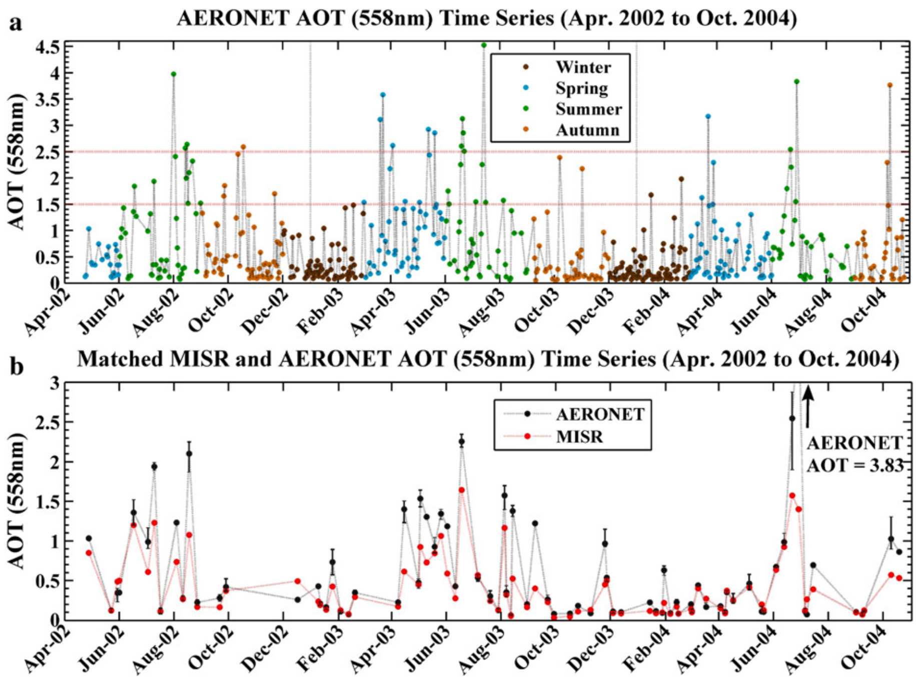

Fig. 3. Time series plots for AERONET and MISR green band AOT during Apr. 2002 to Oct. 2004. (a) All AERONET AOT measurements averaged between universal time 2:00 and 4:00 every day. Points are color-coded by season: spring (blue), summer (green), autumn (yellow) and winter (brown). (b) Matched MISR–AERONET AOT measurements. The vertical bars on the AERONET points show the range of AERONET AOTs in the two-hour averaging window, i.e. the interval between the smallest and the largest AOT.

the green band because all other three band analysis give rises to similar observations of underestimation of AERONET AOT by MISR AOT.

In the scatterplot, the difference between an AERONET AOT and the matched MISR AOT equals the vertical distance from the corresponding point to the 1:1 line. We can see that

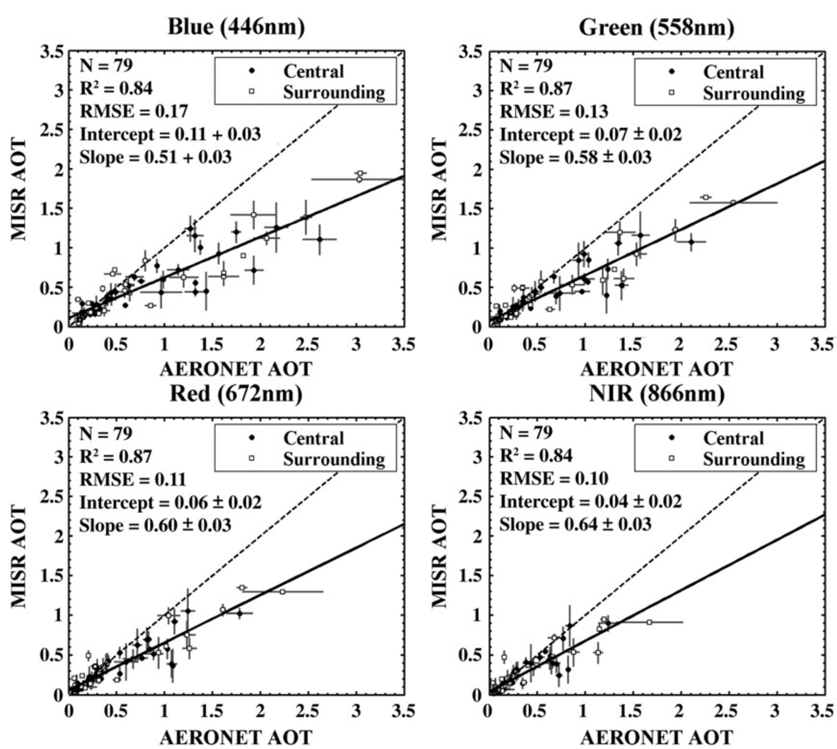

Fig. 4. Scatterplots of MISR versus AERONET AOT in four MISR bands. Four panels represent the blue band, green band, red band and NIR band results, respectively. Central points are marked as solid circles and surrounding points as hollow squares. The linear regression line is shown in solid line, and the dashed line represents the 1:1 line in each subplot. The vertical and horizontal error bars on each point represent the spatial and temporal standard deviations respectively.

when AOT values are small, the differences are mostly small; while when AOT values are large, especially larger than 1.0, differences grow rapidly. This suggests that the agreement between AERONET and MISR deteriorate with increasing AOT. Kahn et al. (2005) found similar results at several urban sites although their AOT values were much lower than those found in Beijing. The authors suggested that an inadequate selection of particle optical models is likely to contribute to the discrepancy, and adding to the algorithm climatology pollution aerosol analogs with lower single scattering albedo (SSA) could raise the AOT and hence better retrieve the particle properties, and it is consistent with our observations of the single scattering albedo (SSA) in the previous section. However, we also find that the points with large MISR–AERONET differences (points that are relatively far away from the 1:1 line) are often accompanied with the long vertical or horizontal error bars, which represent large spatial or temporal variabilities. This indicates that the underestimation may also be possibly caused by spatial or temporal variabilities of aerosols, and brings us to study the impact of these two effects in the next section.

3.3. Impact of temporal and spatial variability of AOT in Beijing

In addition to the lack of appropriate aerosol models, the underestimation of AOT by MISR at high AOT values may also be caused by the temporal and spatial averaging when comparing the snapshots of relatively large areas (i.e., MISR regions) with time-averaged point measurements (i.e., AERONET). For AERONET measurements, averaging in a two-hour window can possibly introduce substantial errors if AOT values vary substantially during that period, and may cause biases if there are no measurements taken close to the time of MISR overpass. To account for this source of uncertainty, the quality assessment (QA) criterion proposed by Diner et al. (2001) is adopted in the current analysis. By implementing a simple temporal analysis on the AERONET data, we find that the standard deviation of AERONET AOT within the two-hour window is about 0.05 on the average, 12% of which is beyond 0.1. To adapt for the situation of high aerosol loading and relatively high temporal variations in Beijing urban environment, a matched point is flagged as "questionable" if the standard deviation of AOT within the two-hour window is greater than 0.1, or no data record is acquired within a 30-minute time window centered at the MISR overpass time. The AERONET AOT values of the "unquestionable" points are averaged within the 30-minute windows, thus are considered to be temporally stable and have a smaller bias. It should be noted that the 30-minute time window varies with the coincident MISR overpass time for each data point.

The 3×3 spatial averaging that has been used in previous validation analyses is also investigated in the current analysis. On one hand, the MISR retrieval uncertainty will probably be reduced due to the 3×3 regions averaging (Martonchik et al., 2004). On the other hand, using AOT values of surrounding regions to estimate the AOT value of the central region within which the AERONET site falls naturally introduces an additional level of uncertainty. Consequently, the central and surrounding points should be treated differently in the linear least squares. In the current analysis, a weighted least squares (WLS) fitting model is explored as an alternative to the traditional least square regression (Weisberg, 1985). Every data point, i.e., a pair of MISR–AERONET AOT values, is now given a weight: for a the surrounding data point, weight is evaluated as the number of the successful retrievals in the 3×3 regions; for a central point, weight is set to 9 to reward its lower bias of spatial mismatch as compared to the surrounding data points.

The agreement between MISR and AERONET AOT is improved when all the temporally "questionable" points were eliminated, as shown in Fig. 5. The ordinary least squares (OLS) fit yields a higher R^2 of 0.94 (equivalent to the correlation coefficient of 0.97), a lower RMSE of 0.08 and a higher slope of 0.71 ± 0.03 (the dashed line in the Fig. 5). The WLS fit, which reduces the impact of spatial variability, yields an even higher slope of 0.73 ± 0.03 (the solid black line in the Fig. 5). This slope is higher than that reported by Kahn et al. (2005) in the continental category (regression slope = 0.68). These noticeable improvements indicate that aerosol temporal and spatial variation can be an important source of uncertainty, and should be considered when validating MISR AOT in the urban environment. By examining several MISR imageries on the dates when AERONET data are highly variable, we find some of them have more cirrus clouds than usual. Therefore, another possible reason may be that some of AERONET observations might include these variable thin clouds, which are excluded from the MISR retrievals through the cloud screening, thus the AERONET AOT would be larger in such cases.

When only the central points (i.e., MISR AOT at the central region matched with AERONET AOT averaged over 30-minute window) are included in the OLS fit, the best agreement with an R^2 of 0.96, a slope of 0.91 ± 0.03, and an intercept of 0.00 ± 0.01 is achieved. Although the regression slope is highly significant (p-value <0.0001), this approach suffers a data loss with only 33 data points remaining, and the AERONET AOT values of these points are all below 1.0 (the original sample size of central points is 48, but some of them are "temporally" questionable, therefore excluded from the analysis). For the central points, MISR AOT is only 9% lower than AERONET AOT on average. This slight underestimation could be due to use of aerosol models with overly large single scattering albedos pointed out in the previous section, or maybe other potential problems of the MISR aerosol retrieval algorithm.

The dramatic improvement of the slope from 0.73 to 0.91, as well as the R^2 from 0.93 to 0.96, suggests that including the surrounding points (the blue squares in the Fig. 5) in the validation process can introduce a substantial low bias. By investigating averaged AOT of the 3×3 regions covering the AERONET site indicated in Fig. 2, we find that all the surrounding regions except one in the southeast have lower values than the central one. To a large extent, this explains the underestimation of AOT by MISR when surrounding points are included. We will go into details on the natural aerosol spatial variation of Beijing in the next section. It should be also noted that in MISR product version 17 and higher, the regional best estimate AOT (MISR parameter name:

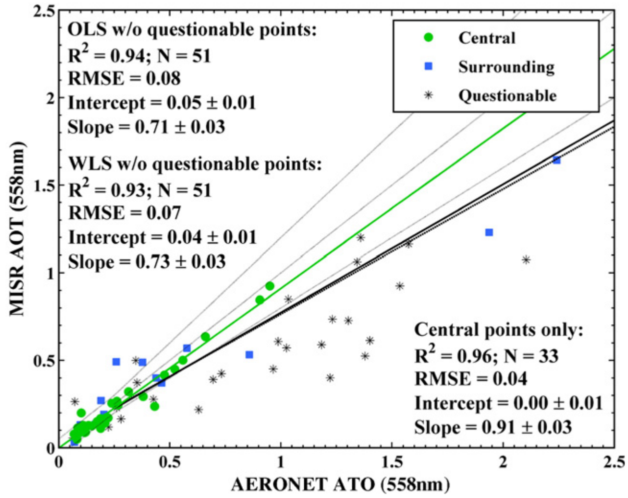

Fig. 5. Scatterplot of MISR versus AERONET green band AOT. "Questionable" points are shown as asterisks. The other "unquestionable" points are shown as green circles for central points and blue squares for surrounding ones. The ordinary least squares (OLS) and the weighted least squares (WLS) fit results are given in the upper left corner of the plot, with the dashed line representing the fitted line of the OLS and the solid black line representing the fitted line of the WLS. The linear regression line for those "unquestionable" central points is shown as the green solid line, with the estimated parameters shown in the lower right corner. The dotted lines represent the 1:1 line and the MISR expected uncertainty envelope for reference.

RegBestEstimateSpectralOptDepth) is the same as the regional mean AOT for a successful retrieval, while in the case of a failed retrieval, the regional best estimate AOT will be filled in with the average of 3×3 successful regional mean AOTs with an associated quality flag. Our finding suggests that special attention should be paid when the regional best estimate AOT is used for aerosol studies in heavily polluted urban environments, because the spatial averaging can possibly introduce bias due to the aerosol spatial variability.

3.4. Indication of spatial variability by ground pollution monitoring data

While the AERONET site in the current study is surrounded by heavy traffic and residential apartments, analysis using geographic information system (GIS) indicates that the MISR regions within which the AERONET site falls covers urban, suburban and rural areas of Beijing. Road and traffic conditions, industrial emission sources, and population distribution are likely to cause the aerosol loadings to vary within these MISR regions. Li et al. (2005b) derived 1-km MODIS AOT data over Beijing urban and suburban area (retrieval errors within 20%). A contour plot of yearly averaged AOT in Li et al. (2005b) showed that the aerosol is highly variable, and the high AOT values are mainly concentrated in the central urban areas with dense population, heavy traffic or industrial emissions. While in this study, we further examine the ground-level PM data to describe the aerosol spatial variation in Beijing.

Although affected by factors such as aerosol vertical profile and particle composition, ground-level particle concentrations are often found to be highly correlated with column particle light extinction properties (Chow et al., 2002; Liu et al., 2005). Due to the lack of long-term $PM_{2.5}$ concentrations data, we use PM_{10} converted from API values as an indicator of the spatial variation of AOT in Beijing. PM_{10} concentrations measured at the Olympic Center, the closest API site to the AERONET site in Beijing were compared with the AERONET AOT measurements. The correlation coefficients are 0.72, 0.61 and 0.59 in the autumn, summer and winter, respectively. The correlation in springtime is weaker (0.32), owing to the long-range transport of Asian dust, which is usually above the boundary layer and therefore not relevant to ground-level PM_{10} concentrations. This reasonably good correlation between PM_{10} concentrations and AOT provides support that the spatial variability of PM_{10} concentrations is a reasonable indicator of the spatial variability of AOT in Beijing area.

Fig. 6 shows the seasonal averaged PM_{10} concentrations in 24 monitoring sites, sorted by the overall mean PM_{10} concentrations. Most of the sites are covered by MISR 3×3 regions used in the current analysis (Fig. 1). PM_{10} concentrations show significant spatial variations across the sites. The spatial standard deviation of daily PM_{10} concentrations among the 24 monitoring sites is 31 μg/m^3, or 23.7% of the mean city-wide PM_{10} concentration. The maximum difference of daily PM_{10} concentrations among the 24 sites is 122 μg/m^3, or 93.6% of the mean city-wide PM_{10} concentration. Overall, PM_{10} concentrations

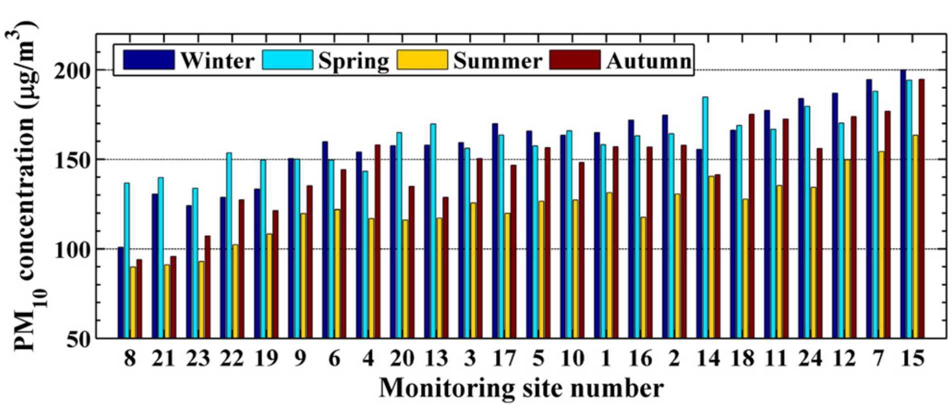

Fig. 6. Bar chart of seasonal average PM_{10} mass concentrations in 24 monitoring sites of Beijing in the year 2003 and 2004. The sites are sorted by their overall mean PM_{10} concentrations and labeled by their site numbers designated in Fig. 1.

exhibit a clear spatial pattern, with lower concentrations in the sites located the northern region of Beijing, such as Dingling (#8), Huairouzheng (#21), Yangqingzhen (#23), and higher concentrations in the sites in the central and southern region. The highest annual PM_{10} concentration is found in the southernmost site Liangxiangzhen (#15) (187 μg/m^3). This is probably because the dominant northerly wind blows polluted air plumes from city center to the suburban and rural areas in the south. Gucheng (#7) and Yuquanlu (#11) sites, which are to the west of the city center and near a major iron and steel manufacturer, also observe very high PM_{10} levels due to proximity to heavy industrial emission sources. These results are consistent with previous findings of the PM spatial distribution in Beijing (Zhao et al., 2004), and also moderately comparable with AOT spatial distribution obtained by Li et al. (2005b). The spatial heterogeneity is more obvious in the summer, autumn, and winter, when local emission sources play a dominant role in determining PM_{10} concentrations. Due to frequent dust storms, PM_{10} concentrations tend to more uniform in springtime (Fig. 6). On average, the daily spatial standard deviation is 20.0% of the mean city-wide PM_{10} concentration in the spring, while 23.6% in the summer, 24.5% in the winter and 26.7% in the autumn.

The heterogeneity of PM_{10} concentrations observed within the MISR regions confirms that averaging of 3×3 MISR regions may introduce substantial uncertainty in MISR AOT validation. The MISR central region (covering the AERONET site) covers most of the heavily polluted central urban area, while some of the surrounding regions extend to suburban or rural areas where the aerosol abundance is substantially lower than the urban center. Regression analysis in the previous section has showed a considerable improvement of the slope from 0.73 to 0.91 when surrounding points are all excluded. Consequently, we believe the 3×3 spatial averaging is one of the main reasons of the MISR's underestimation found in our study. This also suggests that MISR's resolution of 17.6 km may be insufficient to characterize the highly variable aerosol loadings in large metropolitan areas such as Beijing. A finer resolution AOT derived from MISR product would be necessary to better characterize AOT on a local scale. Li et al. (2005a,b) retrieved MODIS AOT at 1-km resolution (10-km in the standard MODIS AOT product) over Hong Kong and Beijing by modifying the MODIS algorithm, and thus better characterize the aerosol spatial variation. Similar approaches could be taken on MISR data.

4. Conclusions

MISR retrieved AOTs are compared with AERONET AOT measurements in Beijing metropolitan area with extremely high aerosol loadings. Data are collected with methods used in previous validation studies by using two-hour temporal averaging for AERONET AOT and both central and 3×3 surrounding averaged retrievals for MISR AOT. When all the matched MISR–AERONET AOT data are included in the analysis, our results show that MISR AOT is strongly correlated with AERONET AOT, but on average is 29% lower. A linear regression analysis using MISR AOT as the response yielded a slope of 0.58±0.03 and an intercept of 0.07±0.02 in the green band with similar results in the other three bands, suggesting that MISR may underestimate AERONET AOT, especially at high AOT values. After applying a 30-minute averaging time window to the AERONET data and controlling their temporal variabilities, the agreement between MISR and AERONET AOT is significantly improved with the correlation coefficient of 0.97 and a slope of 0.71±0.03 in an ordinary least squares fit. A weighted linear least square fit, which reduces the impact of spatial averaging, yields better results with the slope going up to 0.73±0.03. When only the central regions (without 3×3 regions averaging) are used, the best result is achieved with a slope of 0.91±0.03 and an intercept of 0.00±0.01, and the mean MISR AOT of the central regions is only 9% lower than AERONET AOT. By investigating PM_{10} spatial distribution in Beijing, we find substantial spatial variability of aerosol loading with higher PM_{10} concentrations observed in the urban center where the AERONET site is located. When assessed together, the above findings indicate that the substantial underestimation seen in MISR AOT may to a large extent be explained by the low bias introduced by the 3×3 regions spatial averaging. When the temporal and spatial variability of AOT are better controlled, the agreement between MISR and AERONET AOT can be much better than the previously reported results.

In addition, our findings suggest that MISR aerosol retrieval algorithm might need to be adjusted for the high aerosol loadings and substantial spatial variations that it will probably encounter in heavily polluted metropolitan areas. New aerosol mixtures with lower SSAs might need to be introduced to better describe the aerosols present in such environments. The inadequate aerosol models in MISR retrieval algorithm might partially explain the discrepancies as pointed out by Kahn et al. (2005). Further studies are needed to explore alternative statistical methods for MISR AOT validation in order to more accurately characterize the data. With the retrieval algorithm continuously being refined, MISR will provide AOT at higher accuracy. Finally, as the AOT is closely related to PM mass concentration, MISR has the potential capability of assisting in urban air pollution monitoring.

Acknowledgements

This study is supported in part by Microsoft Research Asia, through a research grant to the Microsoft Statistics and Information Technology Laboratory of Peking University. The international collaboration is also supported in part by National Science of Foundation of China (60325101,60628102) and Ministry of Education of China (306017). The work of Bin Yu is partially supported by U.S. NSF Grant DMS-0306508 and U. S. ARO Grant W911NF-05–1-0104. The authors would like to thank Dr. Ralph Kahn and the MISR team for their advice and technical support. We also thank the AERONET PIs Hongbin Chen and Philippe Goloub for theirs effort in establishing and maintaining the Beijing site, and Professor Zhanqing Li for providing source information about the API/PM_{10} data.

References

Abdou, W. A., Diner, D. J., Martonchik, J. V., Bruegge, C. J., Kahn, R. A., Gaitley, B. J., et al. (2005). Comparison of coincident Multiangle Imaging Spectroradiometer and Moderate Resolution Imaging Spectroradiometer aerosol optical depths over land and ocean scenes containing Aerosol Robotic Network sites. *Journal of Geophysical Research-Atmospheres*, *110* (D10), D10S07.

Chow, J. C., Watson, J. G., Lowenthal, D. H., & Richards, L. W. (2002). Comparability between PM2.5 and particle light scattering measurements. *Environmental Monitoring and Assessment*, *79*(1), 29−45.

Christopher, S. A., & Wang, J. (2004). Intercomparison between multi-angle imaging spectroradiometer (MISR) and sunphotometer aerosol optical thickness in dust source regions over China: Implications for satellite aerosol retrievals and radiative forcing calculations. *Tellus. Series B, Chemical and Physical Meteorology*, *56*(5), 451−456.

Chu, D. A., Kaufman, Y. J., Zibordi, G., Chern, J. D., Mao, J., Li, C. C., et al. (2003). Global monitoring of air pollution over land from the Earth Observing System-Terra Moderate Resolution Imaging Spectroradiometer (MODIS). *Journal of Geophysical Research-Atmospheres*, *108*(D21).

Diner, D. J., Abdou, W. A., Bruegge, C. J., Conel, J. E., Crean, K. A., Gaitley, B. J., et al. (2001). MISR aerosol optical depth retrievals over southern Africa during the SAFARI-2000 dry season campaign. *Geophysical Research Letters*, *28* (16), 3127−3130.

Diner, D. J., Beckert, J. C., Reilly, T. H., Bruegge, C. J., Conel, J. E., Kahn, R. A., et al. (1998). Multi-angle Imaging SpectroRadiometer (MISR) — Instrument description and experiment overview. *IEEE Transactions on Geoscience and Remote Sensing*, *36*(4), 1072−1087.

Dubovik, O., Smirnov, A., Holben, B. N., King, M. D., Kaufman, Y. J., Eck, T. F., et al. (2000). Accuracy assessments of aerosol optical properties retrieved from Aerosol Robotic Network (AERONET) Sun and sky radiance measurements. *Journal of Geophysical Research-Atmospheres*, *105*(D8), 9791−9806.

Eck, T. F., Holben, B. N., Dubovik, O., Smirnov, A., Goloub, P., Chen, H. B., et al. (2005). Columnar aerosol optical properties at AERONET sites in central eastern Asia and aerosol transport to the tropical mid-Pacific. *Journal of Geophysical Research-Atmospheres*, *110*(D6).

He, K. B., Yang, F. M., Ma, Y. L., Zhang, Q., Yao, X. H., Chan, C. K., et al. (2001). The characteristics of PM2.5 in Beijing, China. *Atmospheric Environment*, *35*(29), 4959−4970.

Holben, B. N., Eck, T. F., Slutsker, I., Tanre, D., Buis, J. P., Setzer, A., et al. (1998). AERONET — A federated instrument network and data archive for aerosol characterization. *Remote Sensing of Environment*, *66*(1), 1−16.

Jet Propulsion Laboratory (JPL) (2004). Multi-angle Imaging Spectro-Radiometer Data Product Specifications, Revision L: California Institute of Technology.

Kahn, R., Banerjee, P., & McDonald, D. (2001). Sensitivity of multiangle imaging to natural mixtures of aerosols over ocean. *Journal of Geophysical Research-Atmospheres*, *106*(D16), 18219−18238.

Kahn, R., Banerjee, P., McDonald, D., & Diner, D. J. (1998). Sensitivity of multiangle imaging to aerosol optical depth and to pure-particle size distribution and composition over ocean. *Journal of Geophysical Research-Atmospheres*, *103*(D24), 32195−32213.

Kahn, R. A., Gaitley, B. J., Martonchik, J. V., Diner, D. J., Crean, K. A., & Holben, B. (2005). Multiangle Imaging Spectroradiometer (MISR) global aerosol optical depth validation based on 2 years of coincident Aerosol Robotic Network (AERONET) observations. *Journal of Geophysical Research-Atmospheres*, *110*(D10).

Li, C. C. (2002). Remote sensing of Aerosol Optical Depth with MODIS and its application in the regional environmental air pollution studies. Ph.D. thesis, Beijing: Peking University.

Li, C. C., Lau, A. K. H., Mao, J. T., & Chu, D. A. (2005a). Retrieval, validation, and application of the 1-km aerosol optical depth from MODIS measurements over Hong Kong. *IEEE Transactions on Geoscience and Remote Sensing*, *43*(11), 2650−2658.

Li, C. C., Mao, J. T., Lau, A. K. H., Yuan, Z. B., Wang, M. H., & Liu, X. Y. (2005b). Application of MODIS satellite products to the air pollution research in Beijing. *Science in China Series D-Earth Sciences*, *48*, 209−219.

Liu, Y., Park, R. J., Jacob, D. J., Li, Q. B., Kilaru, V., & Sarnat, J. A. (2004a). Mapping annual mean ground-level PM2.5 concentrations using Multiangle Imaging Spectroradiometer aerosol optical thickness over the contiguous United States. *Journal of Geophysical Research-Atmospheres*, *109*(D22), D22206.

Liu, Y., Sarnat, J. A., Coull, B. A., Koutrakis, P., & Jacob, D. J. (2004b). Validation of multiangle imaging spectroradiometer (MISR) aerosol optical thickness measurements using aerosol robotic network (AERONET) observations over the contiguous United States. *Journal of Geophysical Research-Atmospheres*, *109*(D6), D06205.

Liu, Y., Sarnat, J. A., Kilaru, A., Jacob, D. J., & Koutrakis, P. (2005). Estimating ground-level PM2.5 in the eastern United States using satellite remote sensing. *Environmental Science & Technology*, *39*(9), 3269−3278.

Martonchik, J. V., Diner, D. J., Crean, K. A., & Bull, M. A. (2002). Regional aerosol retrieval results from MISR. *IEEE Transactions on Geoscience and Remote Sensing*, *40*(7), 1520−1531.

Martonchik, J. V., Diner, D. J., Kahn, R. A., Ackerman, T. P., Verstraete, M. E., Pinty, B., et al. (1998). Techniques for the retrieval of aerosol properties over land and ocean using multiangle imaging. *IEEE Transactions on Geoscience and Remote Sensing*, *36*(4), 1212−1227.

Martonchik, J. V., Diner, D. J., Kahn, R., Gaitley, B., & Holben, B. N. (2004). Comparison of MISR and AERONET aerosol optical depths over desert sites. *Geophysical Research Letters*, *31*(16), L16102.

Pope, C. A., Thun, M. J., Namboodiri, M. M., Dockery, D. W., Evans, J. S., Speizer, F. E., et al. (1995). Particulate air pollution as a predictor of mortality in a prospective-study of US adults. *American Journal of Respiratory and Critical Care Medicine*, *151*(3), 669−674.

Sun, Y. L., Zhuang, G. S., Ying, W., Han, L. H., Guo, J. H., Mo, D., et al. (2004). The air-borne particulate pollution in Beijing — concentration, composition, distribution and sources. *Atmospheric Environment*, *38*(35), 5991−6004.

Weisberg, S. (1985). *Applied Linear Regression* (pp. 84−92). New York: Wiley.

Zhao, Y., Pan, J., Zhang, H. Y., Guo, J. Y., Wei, Q., & Shi, J. G. (2004). Analysis of inhalable particles pollution in the atmosphere in Beijing area. *Research of Environmental Sciences*, *17*(1), 67−69.